Optimization Methodology for a 2-D Course Correction of a 155 mm Spin-Stabilized Projectile

Guillaume Arnoult, Mickael Zeidler, Eric Garnier

Optimization Methodology for a 2-D Course Correction of a 155 mm Spin-Stabilized Projectile

Guillaume Arnoult,* Mickael Zeidler,†
Nexter Munitions, 18023 Bourges, France

Eric Garnier‡
ONERA - The French Aerospace Lab, 92190 Meudon, France

An optimization methodology applied to the design of a control device on a 155 mm spin-stabilized projectile is presented. The aerodynamic coefficients of a spoiler are estimated from numerical simulations using surrogate models, more specifically kriging and artificial neural network. Interpolations from the surrogate models are coupled with a 6 degrees of freedom flight mechanics code to compute the trajectories of the corrected projectiles. A 2-D correction of the trajectory is produced through the maximization of the Expected Improvement computed from the kriging model of the objective function during the optimization process. Penalty functions are modeled by the calculation of the Probability of Feasibility relying on the kriging estimations of the performances of the projectiles. An analytic optimization problem is firstly resolved by using this methodology which is then applied to the course correction of an artillery projectile. A sequential enrichment of the databases is achieved to increase the accuracy of the response surfaces and determine an optimum to the optimization problem. The geometric characteristics of a spoiler are optimized in order to produce a correction in range and lateral deviation during the flight of the projectile.

I. Nomenclature

alt/alt_{max}	=	Ratio of the altitude over the maximum altitude
D	=	Projectile caliber, m
H_s/D	=	Height of the spoiler based on D
lat/lat_{max}	=	Ratio of the lateral deviation over the maximum lateral deviation
M	=	Mach number
p	=	Number of dimensions of the problem
ran/ran_{max}	=	Ratio of the range over the maximum range
R_{oll}	=	Roll position of the spoiler, deg.
$\hat{s}(x)$	=	Kriging error estimation at point x
S_i	=	Inputs of j^{th} perceptron
S_j	=	Output of j^{th} perceptron
t_d	=	Moment of deployment of the spoiler, s
y_{max}	=	Maximum known value of the function estimated by kriging
$\hat{y}(x)$	=	Kriging estimation of the function at point x
w_{ij}	=	Weights associated to the i inputs of the perceptron
α	=	Projectile angle of attack, deg.
β	=	Bias
ΔC_A	=	Axial force coefficient contribution of the spoiler
ΔC_m	=	Pitching moment coefficient contribution of the spoiler
ΔC_N	=	Normal force coefficient contribution of the spoiler
θ	=	Span of the spoiler, deg.

*Ph.D. student, Département Métier Létalité Aérobalistique, 7, Route du Guerry; guillaume.arnoult@onera.fr
†Research Engineer, Département Métier Létalité Aérobalistique, 7, Route du Guerry; m.zeidler@nexter-group.fr
‡Research Scientist, Department of Aerodynamics, Aeroelasticity and Acoustics, 8, Rue des Vertugadins; eric.garnier@onera.fr

II. Introduction

Control of ammunitions trajectories consists in integrating the ability for a projectile to correct its trajectory during the flight with the aim of reducing the scattering error. In the case of a spin-stabilized projectile, a control system like an isolated spoiler should be freely rotatable relative to the body of the projectile to ensure the ability to correct the trajectory and be adapted for all flight conditions going from high subsonic to supersonic velocities. In order to obtain a 2D correction of the trajectory, meaning a modification in range and lateral deviation, the geometric parameters of the spoiler (the longitudinal position X_s/D w.r.t. the calibre D of the projectile, its height H_s/D and its span θ), its roll position ϕ and its deployment time t_d are the parameters of a surrogate-based optimization. The determination of the trajectory of the projectile relies on the calculation of the aerodynamic coefficients at each time step of the process. Dietrich [1] studied the coupling of a flight mechanic code with aerodynamic coefficients predictions based on calculations of the aerodynamic coefficients of various fidelity. The computations of the coefficients are easily affordable from empirical and semi-empirical models (about 10 min) while the determination using Computational Fluid Dynamics (CFD) requires a month in the case of RANS computations for a 70 s flight trajectory. However, the computations of the coefficients from the empirical models tend to under estimate the axial force coefficient resulting in an extended range and lateral deviation by 3 to 10 % (up to 1200 m in the case of a 12km ranged projectile) compared to the trajectory of the real projectile. Conversely the CFD computations lead to more precise evaluations of the coefficients producing an error of about 2 % on the range and lateral deviation.

Even if CFD evaluations could be used to obtain a precise evaluation of one trajectory of the projectile, an optimization process relying on multiple trajectories computations is not conceivable. Response surface models, also known as surrogate models, offer a solution to reduce the number of CFD computations needed to determine the flight model of the projectile. Instead of computing expensive CFD evaluations over all the flight envelope, the optimization process evaluates a cheap surrogate model from a limited number of expensive calculations of the function and hence reduces the computational cost of the aerodynamic model.

Some comparisons of surrogate models have been achieved for instance by Peter et al [2] where the reconstruction of the total pressure at the exit plane of the stator of VEGA2 is achieved using least square polynomials, artificial neural networks and kriging. The best reconstructions using as few points as possible are obtained with the kriging model and the radial basis function network. A multi-layer perceptron was also evaluated but required much more data to give a satisfactory estimation of the objective function. The same kind of comparison of surrogate models was achieved by Paiva et al. [3] with the aim of optimizing the lift-to-drag ratio of a wing design and the influence of the number of parameters on the performances of the optimizer. In addition, a multi-disciplinary optimization coupling geometric to structural variables was achieved. Initial response surfaces are obtained via kriging, multi-layer perceptron and quadratic polynomials. The optimization converges towards the optimum with the help of an adaptive sampling. Through the different optimizations, the use of surrogate models coupled with an optimization process presents an advantage over classical optimization in terms of function evaluation required to select the optimum configuration.

Optimization based on surrogate models, more especially kriging models, had been conducted several times in the domain of aerodynamics. Simpson et al. [4] compared the performances of surface responses constructed using a polynomial model and kriging to optimize the shape of an aerospike nozzle. The use of a generalized reduced gradient allows determining the shape of the nozzle presenting the maximum thrust over weight ratio. Meunier [5] achieved the optimization of a high lift airfoil equipped with a fluidic flow control in landing conditions. The surrogate model is used to represent the ratio of lift coefficients between the controlled and the uncontrolled airfoil. The optimized configuration is determined by coupling a genetic algorithm to the expected improvement ensuring the convergence towards the final design of the airfoil. A fully reattached flow over the flap was obtained by optimizing the parameters associated to a constant blowing actuator, ensuring the maximum lift in the landing conditions. Kanazaki et al. [6] maximize the lift coefficient of an airfoil at two different flight conditions simultaneously. The kriging model of the lift coefficient is maximized by adding points at the maximum of the expected improvement leading to the determination of the best configuration of flap and slats for the airfoil, taking into account both flight conditions at the same time. Another optimization was led by Jeong et al. [7] with the aim of maximizing the lift to drag ration of a 2-D airfoil, also achieving the localization of promising configurations by the maximization of the expected improvement.

The following sections describe the methodology based on surrogate models, coupling evaluations of aerodynamic coefficients of a control surface with a flight mechanics code. Sections III and IV are respectively dedicated to the presentation of the sampling method and the surrogate models used in the study. Section V presents the kriging and the multi-layer perceptron models constructed from CFD evaluations of the aerodynamic coefficients of the spoiler. The optimization methodology is described in section VI and then applied in section VII where the number of variables

changes between the optimization processes and the impact of the roll position of the actuator is studied.

III. Initial sampling

The quality of the surrogate modelling of a function is determined at first step by the initial sampling plan of the evaluations of the true values of the function. The accuracy of the surrogate model depends on the spreading of these points over the design space. Several methods to spread points over a design space exist: Sobol sequences, Latin hypercube sampling (LHS) or Full Factorial Design are few of them, each one with advantages and drawbacks [8, 9]. In this study, only the Latin Hypercube sampling will be described and used for its simplicity and the good overall performances it offers.

The distribution of N points over an p-dimensional design space using a LHS consists in dividing each dimension of the design space into N non-overlapping equal-probability intervals and then from a user-specified density probability selects one value from each interval in each dimension. A rule a thumb to define the initial number of point in the LHS is to consider $N \in [3^p; 10^p]$ to have a correct initial representation of the function. In the case of CFD evaluations for the modelling of aerodynamic coefficients for instance, the number of sampling points is greatly reduced due to the computational cost of 1 calculation. From a practical point of view only the spreading of 3^p points will be considered to establish a kriging database.

The optimization of the distribution of the points in the design space is achieved using the Morris and Mitchell criterion [10] which maximizes the minimal distance between the sampling sites. This criterion allows obtaining homogeneous distribution over the design space leading to sampling plans offering a better initial guess of the function than an unoptimized LHS.

In the present study an adaptive sampling is considered meaning that new evaluation points will be regularly added to the initial database to improve the quality of the surrogate model leading to a more accurate representation of the function.

IV. Overview of the surrogate models

A. Kriging

Kriging is a method originally applied by D. G. Krige for the search of ore localization in the 1950's. It was then described mathematically by Matheron who gave the name to the method in tribute to his founder. The demonstration of the results of the kriging is proposed by Jones et al [11]. The estimation of an unknown function is determined from the combination of the mean of the model μ and a statistical deviation $Z(x)$. The estimation of the function at an unknown point (x) is given by the relation

$$\hat{y}(x) = \mu + Z(x) \tag{1}$$

where the statistical deviation is characterized by a zero mean and a covariance between $Z(x_i)$ and $Z(x_j)$

$$COV(Z(x_i), Z(x_j)) = \sigma^2 . R(f(x_i, x_j)) \tag{2}$$

with σ^2 the variance of Z and R the correlation matrix. f is a correlation function defined by the user and determined from the N original sample points which depends on a weighted distance between the points.

$$d(x_i, x_j) = \sum_{k=1}^{p} \theta^k |x_i^k - x_j^k|^2 \tag{3}$$

where θ is an hyperparameter of the surrogate model and is optimized using the Maximum Likelihood Estimate. This parameter is associated to the influence of the variable, as on high values of θ means that there is a low correlation between points. In contrary a low value of θ would mean that the values of the function across the x_i points are very similar.

The Gaussian correlation function is defined, using the distance function

$$R(\theta, x_i, x_j) = exp\left(- \sum_{k=1}^{n} \theta |x_i^k - x_j^k|^2 \right) \tag{4}$$

The determination of the hyperparameter θ is achieved through the maximization of the likelihood function (Sacks et al. [12])

$$MLF = max\left(-\frac{N}{2}ln(\hat{\sigma}^2) - \frac{1}{2}ln(|R|)\right) \tag{5}$$

where

$$\hat{\sigma}^2 = \frac{(y - 1.\mu)R^{-1}(y - 1.\mu)}{N} \tag{6}$$

1. denotes a N-vector of one. This maximization is an iterative step of the construction of the Kriging model, hence computationally expensive due to the multiple matrix inversion required. Now that the hyperparameters are estimated, the function values at an unknown point x can be evaluated

$$\hat{y}(x) = \hat{\mu} + r^T R^{-1}(y - 1.\hat{\mu}) \tag{7}$$

with r a N-vector of the correlation between the estimated error at unknown point x and the error terms at the sampled points and with

$$\hat{\mu} = \frac{1^T R^{-1} y}{1^T R^{-1} 1} \tag{8}$$

The main advantage of the kriging over others surrogate models is its ability to provide an estimation of the function and the error associated to the prediction

$$s^2(x) = \sigma^2\left[1 - r^T R^{-1}.r + \frac{(1 - 1^T.R^{-1}.r)^2}{1^T R^{-1} 1}\right]^{1/2} \tag{9}$$

B. Artificial Neural Network

Artificial Neural Networks (ANN) were firstly described by McCulloch and Pitts in 1943 [13]. The architecture of ANN relies on the interconnections of neurons (known as perceptrons) which are composed of two elements: a weighted summation of the inputs and an activation function. The activation function may be of any kind of linear function but the most commonly used is the logistic function

$$f(x) = \frac{1}{1 + e^{-x}} \tag{10}$$

The Multi-layer perceptron (MLP) is one particular architecture of the ANN in which multiple layers of perceptrons are connected, as it is illustrated in fig. 1.

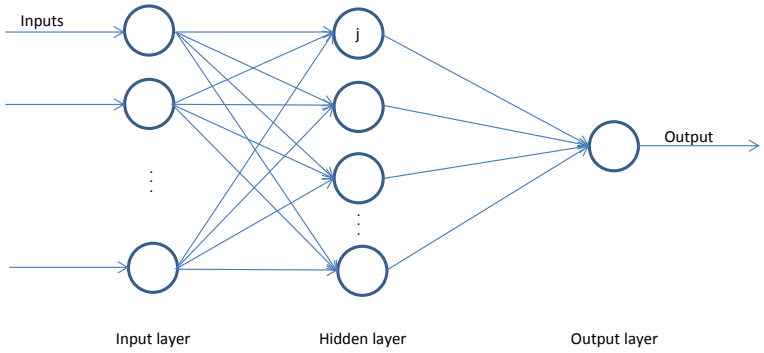

Fig. 1 Architecture of a Multilayer perceptron

The output of the j perceptron is computed as

$$S_j = \sum_{i=1}^{n} w_{ij} s_i + \beta \tag{11}$$

where w_{ij} are the weights associated to each inputs of the j perceptron, s_i are the inputs of the perceptron and β is a bias.

The weights allocated to each perceptron of the MLP are defined during the training phase of the surrogate model using a backpropagation algorithm. Their determination is achieved in order to minimize the error between observed values and estimated outputs. This minimization is achieved with a stochastic gradient descent which modifies the weights at each iteration of the training process

$$w \leftarrow w - \alpha \frac{\partial e(w)}{\partial w} \tag{12}$$

where α is the learning rate and $e(w)$ is the error.

C. Optimizer

To determine which trajectory should be computed accurately, a genetic algorithm (GA) is employed. GAs are selected because of their robustness for aerodynamic problems where nonlinearities and discontinuities may be faced. Moreover GAs start the search for the optimum from a population of points that are not meshing the design space but allow a continuous search. The population size is set to 80 while the number of generations depends on the convergence of the best individual over the last 150 generations.

In the present study, a bi-objective optimization is considered. This kind of optimization has been handled with a genetic algorithm developed by Deb et al. [14]. The nondominated sorting genetic algorithm II (NSGA-II) is able to find solutions belonging to the Pareto front. At each generations all the individuals are ranked, the non-dominated solutions are assigned rank one while the rest of the population is sorted and the individuals now dominating are assigned rank two and so on until the whole population gets a rank. The multi-objective optimization is thus reduced to a single objective minimization of the rank of the individuals. This particular genetic algorithm was applied with success to various optimization problems (zdt1 to zdt6 problems defined by Deb [15]) based on surrogate modelling by Voutchkov and Keane [16].

V. Estimations of the aerodynamic coefficients of the spoiler

The aerodynamic conditions during the flight of the projectile are ranging from the high subsonic (at the end of the flight) to supersonic ($Mach = 2.74$ at the firing). A control surface would preferably be deployed in the second half of the flight (once the apogee is past) allowing to acquire the most information about its trajectory and should therefore be adapted for high subsonic to low supersonic conditions. Surrogate models were used to approximate the aerodynamic coefficients of the spoiler (ΔC_A for the additional axial force coefficient, ΔC_N for the additional normal force coefficient and ΔC_m for the additional coefficient of momentum).

The pressure fields around the projectile and the projectile with the control device are presented on fig. 2 and 3. These results are obtained from Reynolds Averaged Navier-Stokes (RANS) one equation turbulence model of Spalart-Allmaras (SA) computations. On both figures the iso-contour of pressure are presented with the streamlines for computations at a Mach number of 0.984 and an angle of attack of 5.3°. The evolutions of the pressure coefficient along the projectile body are presented on fig. 4 and 5.

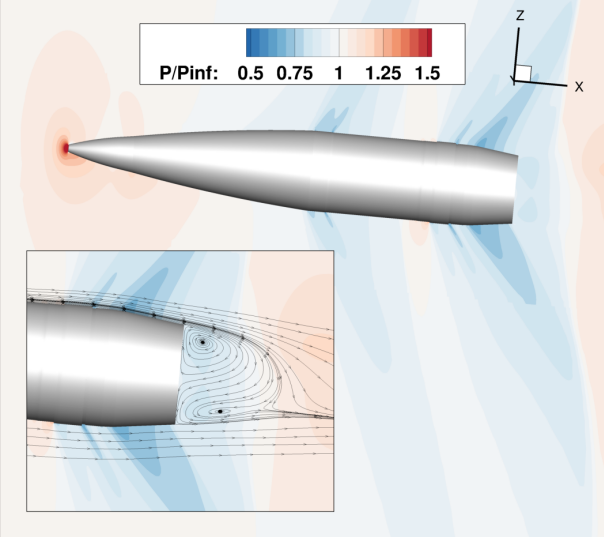

Fig. 2 Pressure field around the body of the projectile, $M = 0.984$ and $\alpha = 5.3°$

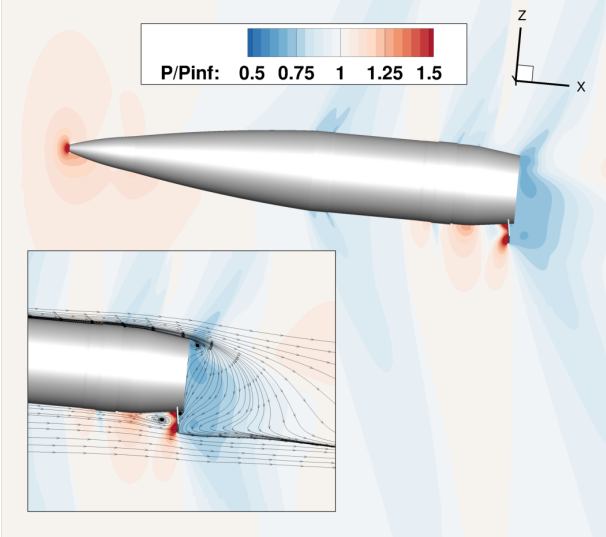

Fig. 3 Pressure field around the projectile equipped with a spoiler, $M = 0.984$ and $\alpha = 5.3°$

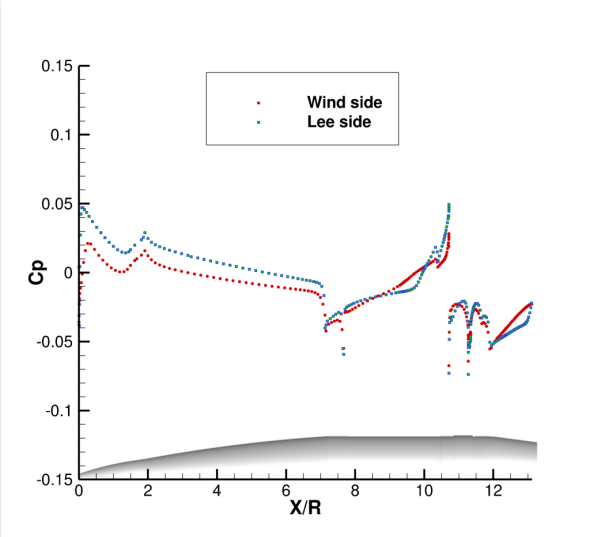

Fig. 4 Longitudinal evolution of the pressure coefficient of the projectile, $M = 0.984$ and $\alpha = 5.3°$

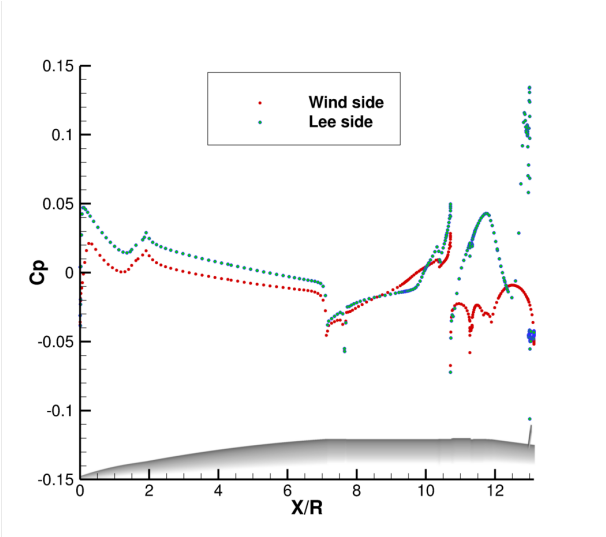

Fig. 5 Longitudinal evolution of the pressure coefficients of the projectile equipped with a spoiler, $M = 0.984$ and $\alpha = 5.3°$

The main characteristics of a transonic flow field were described by Simon [17] who studied the unsteady flowfield around the projectile without control. The flow is firstly accelerated along the ogive of the projectile which is characterized by a decrease of the pressure coefficient until the junction with the cylinder. A first shock appears at this junction and another one is present at the junction between the cylinder and the boat tail. At each geometric junction a rapid change in the pressure profile can be noticed. The zoom presented on fig. 2 evidences the recirculation bubble behind the base of the projectile. Due to the angle of attack of the computation, the two parts of the bubble are not symmetrical about the projectile revolution axis. The stagnation point is thus displaced to the pressure side of the projectile compared to the position of the stagnation point of a simulation at a 0° angle of attack as presented in [17] at various Mach numbers. The presence of the spoiler has a 3D influence on the flowfield and modifies the pressure repartition on both sides of the projectiles. The pressure in the lee side of the projectile is slightly increased as shown by the evolution of the C_p on fig. 5. The most important modification is noticeable in the pressure side of

the projectile with the increase of the pressure just ahead of the spoiler. A recirculation bubble is evidenced by the streamlines on fig. 3. Between $11 \leq X/R \leq 12$ the spoiler has an important influence on the pressure field which values are greatly increased, decreasing the velocity of the flow. Concerning the base flow of the controlled projectile, it is greatly influenced by the presence of the spoiler since the recirculation bubble seems to have disappeared, only a small bubble remains at the lee side.

For each flight condition the aerodynamic coefficients of the body of the projectile and of the projectile equipped with a spoiler are computed. The aerodynamic coefficients of the spoiler (ΔC_A, ΔC_N and ΔC_m) are obtained from the difference between the coefficients of the controlled and the uncontrolled configuration once a converged state of the computation is reached.

The 2D course correction of the projectile is a combination of range and lateral deviation modifications. In the case of a gyrostabilized projectile, the lateral deviation is a function of the ratio: $\Delta Z = f\left(\frac{C_{N\alpha}}{C_{m\alpha}}\right)$ described in eq.13.

$$\begin{aligned} \Delta Z &\approx \int_{t_{vol}} \left(\int_{t_{vol}} \frac{L_\beta}{m} dt \right) dt \\ L_\beta &= \frac{1}{2} \rho_a S V^2 C_{n_\alpha} sin(b) \\ b &\approx \frac{2gcos(\theta)}{SD} \frac{p}{V^3} I_1 \frac{1}{C_{m\alpha}} \frac{1}{\rho_a} \end{aligned} \tag{13}$$

It is easily understandable that to maximize the ΔZ, the ΔC_{N_α} should be maximized and the ΔC_{m_α} minimized, what would be produced by a spoiler situated close to the aft of the projectile (the C_{m_α} is therefore opposed to the incidence of the projectile and negative). The determination of the aerodynamic coefficients depends on the geometric characteristics of the spoiler with respect to the calibre of the projectile and on the flight conditions: longitudinal position from the nose of the projectile X_s/D, height of the spoiler H_s/D, the span θ, the Mach number M and the angle of attack α. The interested reader in the correction of the course of a projectile by a spoiler is referred to [18] and [19].

2 response surfaces were constructed from the CFD computations, one using MLP and the other considering kriging for each aerodynamic coefficient of the spoiler (ΔC_A, ΔC_N and ΔC_m). 1300 CFD calculations of the projectile with a spoiler were computed however only 243 (= 3^5 samples) configurations followed the LHS spreading rules. To avoid overfitting, and therefore a deterioration of the quality of the kringing model, only these 243 samples were used to construct the response surfaces with kriging while the 1300 calculations were taken into account in the case of an MLP. The quality of the response surface was evaluated over a validation set independent from the training set. These verifying points are sampled using an LHS in order to be sampled over the entire 5-dimensional space domain. In spite of the difference in the quantity of points used to elaborate the different response surfaces, the estimations of the normal force coefficient are presented on fig. 6 and 7 were it appears that the meta models present almost the same quality over the validation set.

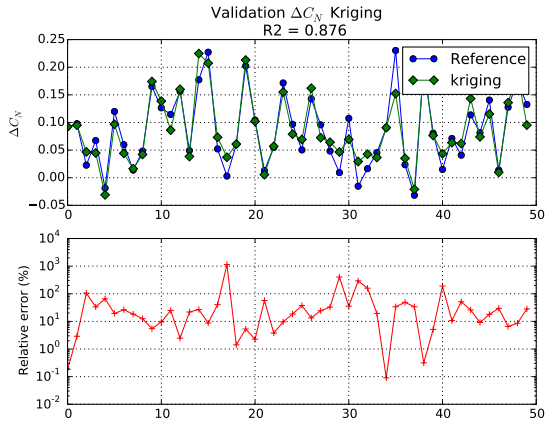

Fig. 6 Estimation of the normal force coefficient by kriging over the validation set

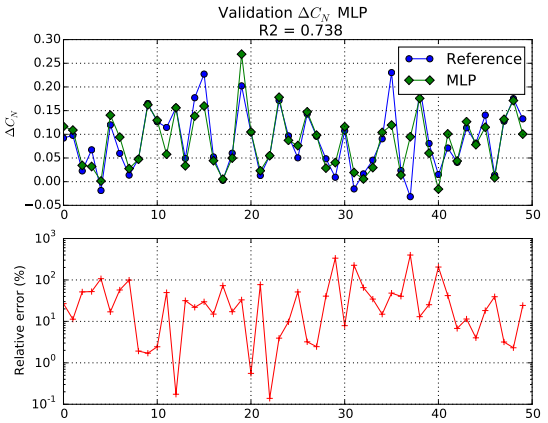

Fig. 7 Estimation of the normal force coefficient by MLP over the validation set

High values of the relative error are generally associated to low values of the aerodynamic coefficient evaluated, indeed an estimation of a very low 'true' value of C_N as it is shown in fig. 6 and 7 leads to high values of the relative error associated. The evaluation of the estimations quality of both surrogate models is measured using the coefficient of determination R^2

$$R^2 = 1 - \frac{\sum_{i=1}^{M}(\hat{y}(x_i) - y(x_i))}{\sum_{i=1}^{M}(y(x_i) - \bar{y}(x))} \tag{14}$$

where $\hat{y}(x_i)$ is the estimation by the surrogate model at sample x_i, $y(x_i)$ is the value of the coefficient evaluated by CFD and $\bar{y}(x_i)$ is the mean over the N samples of the validation set. The estimations of the kriging model are closer to the true values of the normal force coefficient over the validation set than the MLP estimations. Even if the sampling plan used to construct the kriging model is reduced compared to the number of computations used for the construction of the MLP, kriging is able to reproduce the variations of the aerodynamic coefficients in unexplored area with more accuracy.

VI. Description of the optimization procedure

The algorithm followed to determine the optimum configuration of the spoiler is described in fig. 8. The objective of the optimization procedure is to identify the configurations of the spoiler producing a 2D course correction of the projectile.

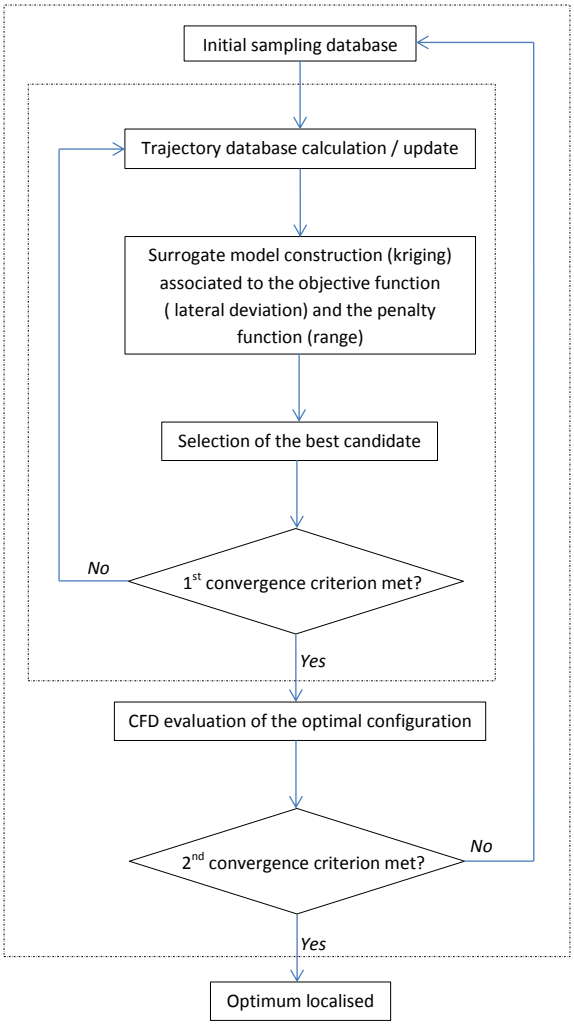

Fig. 8 Outline of the surrogate-based optimization algorithm

5 design parameters corresponding to the geometric characteristics of the spoiler and to its deployment during the flight are optimized.

- The longitudinal position of the spoiler X_s/D defining the magnitude of the pitching moment of the spoiler. In all cases, the application point of the normal force produced by the spoiler is located behind the center of gravity of the projectile. The resulting pitching momentum is therefore negative and opposed to the angle of attack of the projectile for a spoiler located below the projectile. It is expected that the optimized spoiler will be close to the aft of the projectile considering eq. 13.
- The height H_s/D and the span θ are defining the frontal surface of the spoiler. Their combination defines directly the drag contribution of the spoiler.
- The deployment time t_d determines at which flight point the spoiler is deployed and thus the magnitude of the correction.
- The roll position ϕ defines toward which direction the course correction will result. For instance if $\phi = 0°$ the spoiler is located below the projectile. The force produced is directly opposed to the position of the spoiler and will result in an increase in range.

The variation ranges of the parameters are gathered in table 1.

	Optimization range	
	min	max
Longitudinal position X_s/D	4.85	5.5
Height of the spoiler H_s/D	0.05	0.25
Span of the spoiler θ (°)	15	60
Moment of deployment (s)	45.44	102.29
Roll position ϕ (°)	0	360

Table 1 Optimization parameters range

The initial conditions for the reference projectile are an initial velocity of 933 m/s and an initial roll speed of 301.06 tr/s. These conditions lead to the trajectory of an uncontrolled projectile illustrated on fig. 9. At the impact point are also plotted the standard deviations associated to the total error and corresponding to 2σ in range and lateral deviation since it is assumed that the dispersion follows a Gaussian distribution around the mean point.

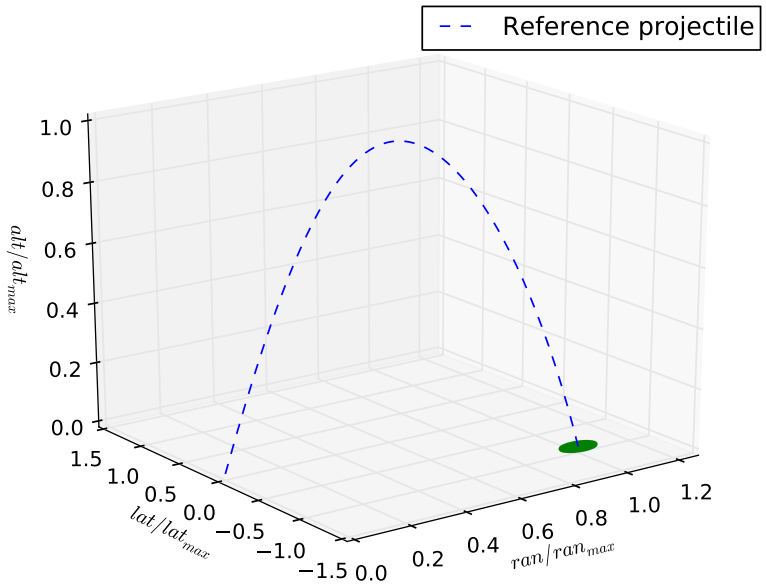

Fig. 9 Trajectory of the reference projectile

A. Surrogate modelling of the objective and penalty functions

The objective function of the optimization process is defined as the distance between the impact point of a controlled projectile and the nearest point belonging to the 3σ ellipse. Following this function, it is ensured that the selected configuration would be able to produce a course correction for a maximum of trajectories (the 3σ ellipse is a representation of the Gaussian distribution of the impact points then more than 99% of these points are expected to be localized inside this ellipse). However not all the spoiler producing a correction would be considered as local optimum. To reduce the possibilities and thus converge toward an optimum configuration, penalty functions are introduced into the definition of the optimization problem. These penalty functions are modelled following the definition of the Probability of Feasibility (PF) introduced by Schonlau [20] and applied to an optimization based on surrogate models by Parr et al. [21]. In the same way as for the EI, the PF takes advantages of the kriging modelling of a function to estimate if constraints are respected, see eq. 15.

$$P[F(x)] = \frac{1}{\hat{s}(x)\sqrt{2\pi}} \int_0^{\infty} e^{-[(G(x)-g_{min})-\hat{g}(x)]^2/(2\hat{s}(x))^2} dG \tag{15}$$

where g is the constraint function, g_{min} is the limit of the constraint and $G(x) - g_{min}$ is a measure of the feasibility.

The EI score of each individual of the population is multiplied by the estimation of the PF associated for each constraint. In the present case 3 constraints are modelled and will be described in paragraph VIII A. The initial response surfaces are constructed from samples spread over the $p = 5$ dimensional domain considering an optimized LHS. The number of samples is directly determined from the rule of thumb stated earlier as 3^p. The trajectories of the initial 5-dimensional sampling are computed using the 6-DOF flight mechanics code Balco [22] and are presented on fig. 10. The variety of the configurations obtained via LHS allows determining an initial response surface to start the optimization process.

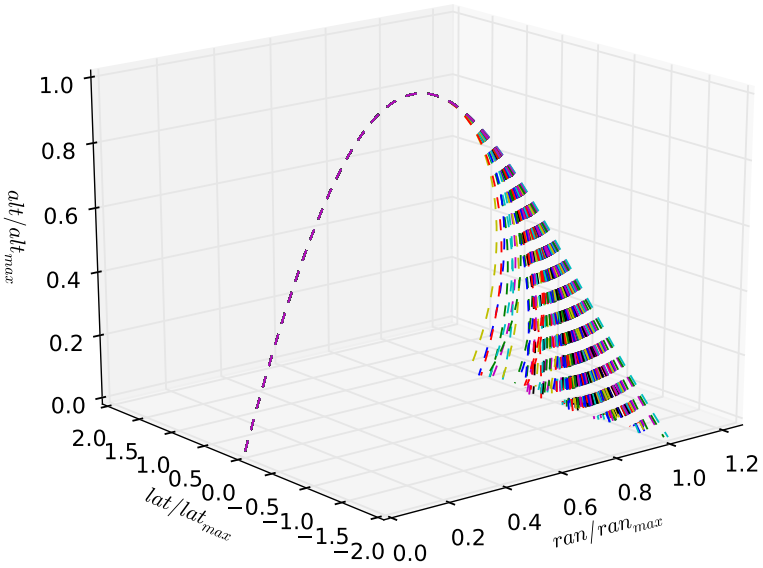

Fig. 10 Trajectories of the configurations determined by a 5-dimensional LHS

B. Selection of best candidate

The elaboration of a kriging surrogate model gives estimations of the values of a function and an estimation of the associated error at unknown points. These information is used to define the Expected Improvement (EI) introduced by Jones et al. [11] which is the mathematical translation of the probability that an unevaluated point perform better than the already known maximum of the function.

$$E[I(x)] = (\hat{y}(x) - y_{max})\Phi\left(\frac{\hat{y}(x) - y_{max}}{s(x)}\right) + s(x)\phi\left(\frac{\hat{y}(x) - y_{max}}{s(x)}\right) \tag{16}$$

where Φ and ϕ are respectively the cumulative distribution and the standard normal density function. The maximization of this function is achieved by using a genetic algorithm. The EI proposes a trade-off between the exploration and the exploitation of the surrogate model. Indeed, the values associated to the EI score are high in the regions of the design space where the function values are significant (exploitation of the model) but are also high in the unknown regions of the model where the error associated to the model $s(x)$ are large (exploration).

At this point of the optimization, the surrogate model associated to the range reached by the projectile is used to lower the EI of the configurations that do not fulfil the range criterion established earlier. However, mostly at the beginning of the optimization process, some of the evaluated configurations are selected even if they finally do not meet the criterion. It is due to the fact that the response surface used to estimate the range of these projectiles is not accurate enough at the beginning of the process but gain in precision, since at each iteration of the optimization process, new data is added to the objective function and the range databases.

C. Estimation of the quality of the response surface

The values of EI do not strictly decrease when points are added to the database, as it has been shown by Forrester and Keane in [23]. When a local optimum is located by the kriging, the values of the kriging tend to reduce while they

tend to increase when another promising zone of the design is located. To determine if the optimization is converged and if the optimal configuration of the spoiler is localized, the accuracy of the response surface associated to the objective function is assessed. To quantify the quality of the response surface, a *Leave One Out Cross Validation* (LOOCV) is calculated. It is evaluated as the 1*st* convergence criterion of fig. 8 and compared to a threshold below which the response surface is considered inaccurate to localise the optimum configuration of the projectile.

The *LOOCV* method consists in removing one-by-one each point of the N sampling points to construct N new response surfaces from the degraded sampling of N-1 remaining points. The mean squared error between true value of the function and the estimation returned by the degraded response surfaces is evaluated. An important error shows a lack of robustness of the surrogate model and additional points are needed to outline the evolution of the function in this zone. However since the process may be very time-consuming and computationally expensive, depending on the number of points in the database, the LOOCV is calculated only every 50 iterations.

D. Evaluation of the aerodynamic coefficients of the optimal spoiler

Once the optimization budget is reached, the aerodynamic coefficients of the local optimum configuration are computed using elsA CFD solver of Onera. The spoiler is associated to the mesh of the body of the projectile using the Chimera method allowing to merge different meshes into a unique one. The aerodynamic coefficients of the spoiler are added to the database to refine the response surface in the zone of interest. The flight conditions at which the configuration is evaluated are chosen according to the flight envelope determined by the flight mechanics code. To ensure that the computations are meaningful, a LHS is used to define the aerodynamic conditions of the calculations. A variable number of new coefficients is added to the database at each enrichment step of the optimization as illustrated in fig. 11 where the new calculations points in red are spread along the trajectory once the spoiler is deployed.

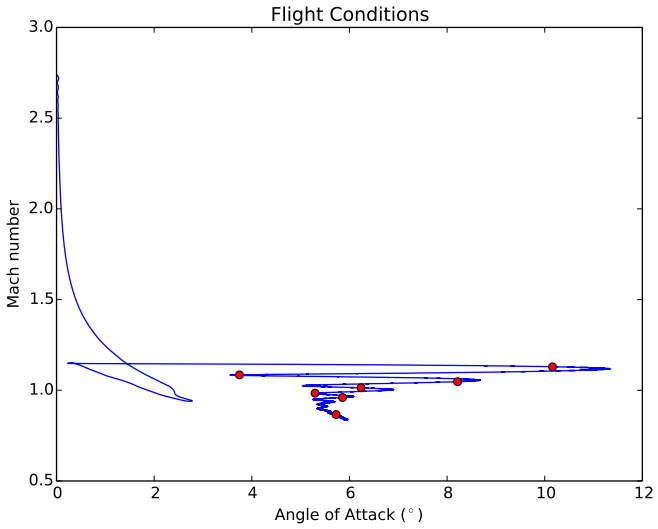

Fig. 11 Calculation points for the refinement of the aerodynamic coefficients response surfaces

The enrichment of the aerodynamic coefficients databases is necessary to increase the accuracy of the surrogate model. The initial response surfaces may not be locally accurate enough to identify the global optimum of the function and to ensure that the optimizer has not selected a 'false' optimum.

VII. Application to an analytic constrained problem

The performances of optimization algorithms, based on surrogate models like in the present case, is usually tested on analytic problems. Most of the times these problems present a large number of local optimum but only one global optimum like it is the case for Rastrigin or Griewank functions. The algorithms are also tested on constrained problems like the one defined by Sasena [24] which was solved by Durantin et al. [25] using a kriging modelization of the objective function :

$$min f(x) = -(x_1 - 1)^2 - (x_2 - 0.5)^2 \tag{17}$$

and of the constraints :

$$\begin{aligned} g_1(x) &= \left[(x_1 - 3)^2 + (x_2 + 2)^2\right] e^{-x_2^7} - 12 \leq 0 \\ g_2(x) &= 10x_1 + x_2 - 7 \leq 0 \\ g_3(x) &= (x_1 - 0.5)^2 + (x_2 - 0.5)^2 - 0.2 \leq 0 \end{aligned} \tag{18}$$

The function without any constraint is presented in fig. 12and the addition of the constraint functions to the initial problem lead to the representation of fig. 13. The interval of definition of the function is now reduced and the function presents one local optimum in (0.2316;0.1216) and one global minimum located (0.2017;0.8332) which value is -0.7483 represented by the blue dot in fig. 13. The interest for the algorithm is to localized the two zones presenting low values of the function and being able to localize the global optimum. To this end an initial sampling of Sasena's function eq. 17 is defined by LHS. A first estimation of the objective and of the constraint functions is obtained and the optimization process can initialize the search for the solution of the optimization problem.

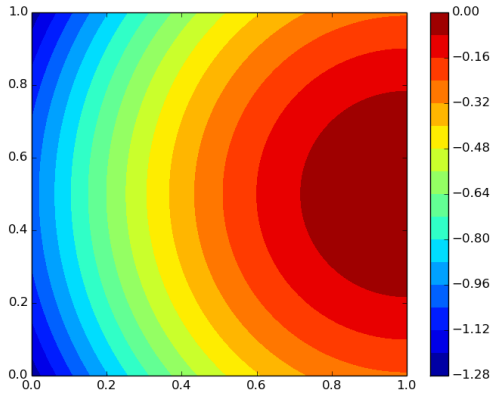

Fig. 12 Sasena's function without constraints over $[0; 1]^2$

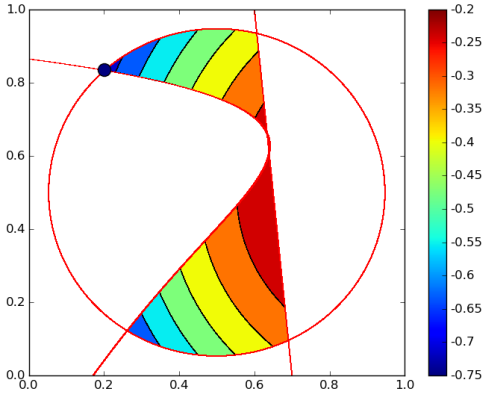

Fig. 13 Constrained Sasena's function, the red lines are the edges of the constraints

Finally, the adaptive sampling leads to the result presented in fig. 14 after 100 new points were added to the initial sampling. The two promising zones are clearly identified by the process and the new samples are concentrated around the low values of the functions, while the constraints are well estimated and respected in the selection of new sampling points. The solving process which was detailed earlier and applied here is promising and will now be applied to the course correction of the projectile.

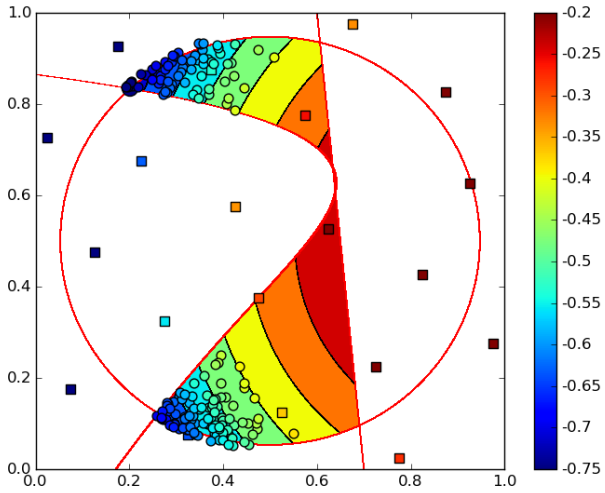

Fig. 14 Minimization of the Sasena's function, initial sampling in squares, adaptive sampling in circles filled by the value of the function

VIII. Application to the course correction of a gyrostabilized projectile

A. Definition of the objective and penalization function

In the case of the projectile, a control device able to produce a 2D course correction is designed and its geometric parameters are optimized. The correction should be produced in the mean time in range and lateral deviation. The roll position of the spoiler determines in which direction an additional force is applied to the projectile which is also the direction of the modification of the trajectory. The minimum objective in terms of correction of the trajectory is 2σ which corresponds to an ellipse around the mean impact point. Considering a Gaussian distribution around this mean impact point, the maximum correction of the trajectory is fixed to 3σ corresponding to a correction of more than 99% of the uncontrolled trajectories. This upper limit is fixed to avoid an oversizing of the dimensions of the spoiler and is integrated in the process as a constraint function. The position of the impact point of a controlled configuration is compared to the distance between the nearest point on the 3σ ellipse and the mean impact point of the reference projectile. The minimization of this distance is the objective function of the process.

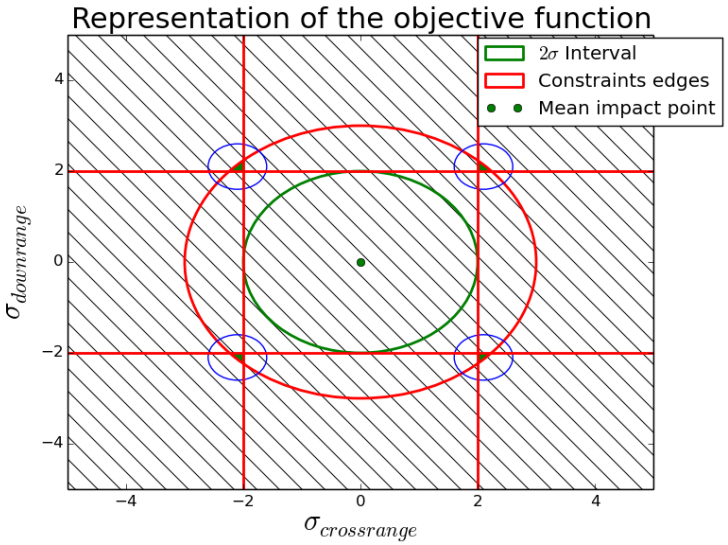

Fig. 15 Objective function of the optimization process, the constraints are the red lines, the hatched zones are the not respected constraints zones

These considerations lead to the definition of the objective function presented in fig. 15. The hatched zones represents where the constraints are not respected. Finally only 4 zones correspond to a 2D correction and are circled in blue. An additional step to simplify the optimization is to consider the characteristics of the uncontrolled projectile. Firstly the projectile is gyrostabilized, it has a positive rotational speed around its revolution axis which produces a natural lateral deviation during the flight oriented to the right. The optimization problem is simplified to consider only the less favorable situation. Then the two zones located on the right of the mean impact points are not considered as a target for the optimization. Additionally the deployment of the spoiler leads to an increase of the drag coefficient of the configuration thus the reduction of the range is easily produced by the spoiler however an increase in range is more difficult to obtain. Finally, for the optimization process, only the zone located on the upper left quarter is considered, corresponding to an increase in range and a diminution of lateral deviation against the natural motion of the projectile.

B. Reduction of the number of parameters

A first optimization was ran with the 5 parameters described in table 1. The results of this optimization phase are presented in fig. 16.

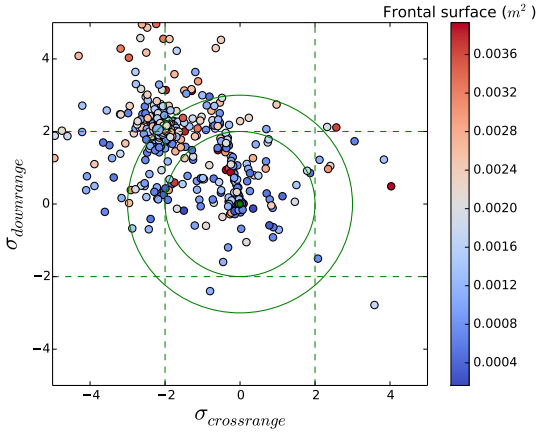

Fig. 16 Positions of all the impact points of the optimization process

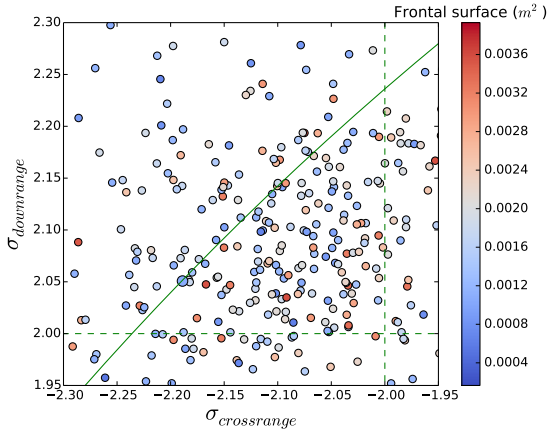

Fig. 17 Zoom on the interest zone of optimization

It appears that the first sampling of trajectories is not sufficient to directly select configurations of the spoiler leading to impact points localized in the area presented in fig. 17. The exploration part of the EI selects configurations of the spoiler which produce an insufficient correction of the trajectory until the response surface is sufficiently accurate to localize the interesting configurations. Finally the results are presented in fig. 17. It can be noticed that a great variety of configurations are producing a 2D correction of the trajectory. The dots are coloured by the frontal surface of the spoiler. Small spoilers were promoted during this first computations coupled with an early deployment time so the integral of the additional normal and lateral forces generated by the spoiler are maximized. However even after some CFD enrichment of the aerodynamic coefficients databases the optimization process did not converge toward a unique solution. Actually after these steps, it was concluded that the frontal surface leading to a 2D correction of the trajectory was defining an iso-surface in the 5 dimensional space of parameters. The value of the reference surface is fixed by the deployment time and any combination of the span θ and the height H_s/D resulting in this value could lead to a 2D correction. The issue is that this time is a parameter of the optimization and varies from an iteration to the other during the determination of an optimum spoiler.

The optimization was not closed and an additional constraint was needed. The terminal guidance of the projectile was considered and it was decided to deploy the spoiler 13.075 s before the impact of the reference projectile.

C. Optimization of the geometric parameters of a spoiler for a fixed deployment time

The methodology presented in paragraph VI is applied to the optimization problem with only 4 parameters since the deployment time of the spoiler is now fixed. The process is initialized from $3^4 = 81$ trajectories used to model the objective function. A first estimation of the constraints is also determined from these calculations.

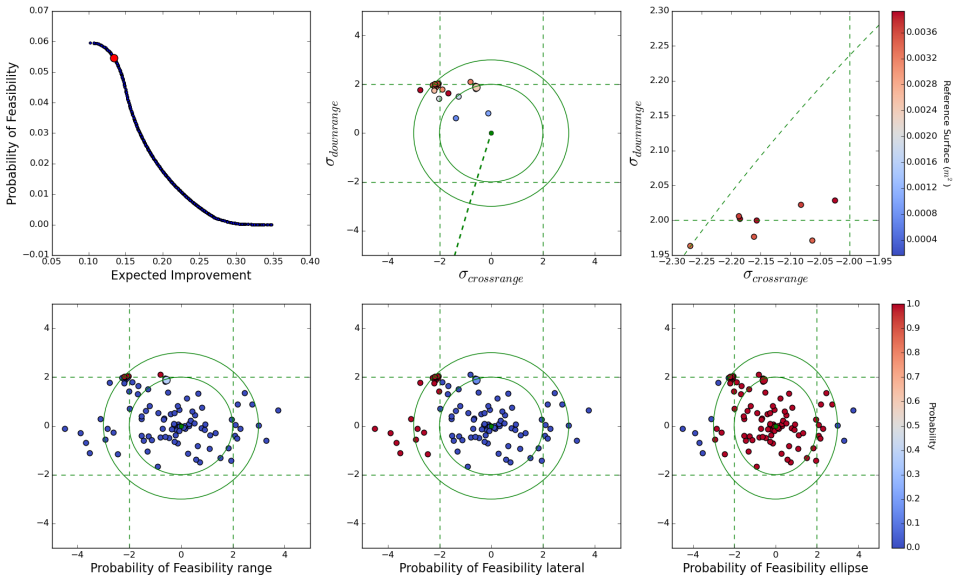

Fig. 18 Evaluation of the Pareto Front and of the constraint functions during the optimization process

The plot of the on-going optimization is presented on fig. 18 detailed with the evaluations of the constraints and the Pareto Front. The Pareto Front is presented on the left of the first row. The configuration selected by the algorithm is the one presenting the maximum value of the product $EIxPF$ highlighted in red. The corresponding impact point is drawn in the figure in the middle of the first row on which are also represented the mean impact point and its trajectory in bold dashed line. The constraints are modelled by the dashed vertical and horizontal lines while the 2σ and 3σ ellipses are in green.

The figure on the lower row are the representation of the different constraint functions. They are well taken into account by the optimization process as the values of the sampling are set to 0 when the constraint is not respected and is 1 when the impact point fulfils the criteria.

Contrary to the preceding optimization step, the algorithm localized promising configurations of the spoiler rapidly and seems to enrich the response surfaces mainly in this interesting area. As expected the frontal surface of the spoiler leading to impact points located in the objective area is constant, the difference in positioning is due to the roll position ϕ of the spoiler. The final results of the optimization is presented in fig 19.

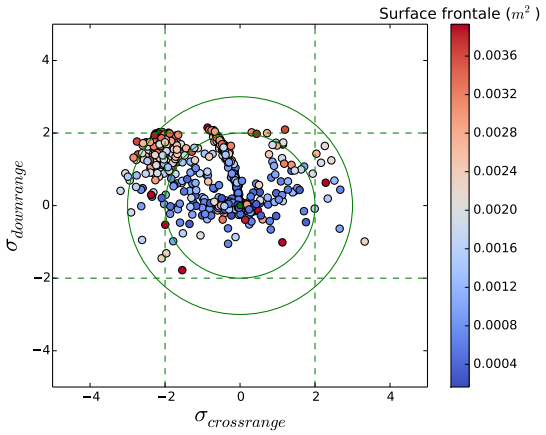

Fig. 19 Positions of all the impact points of the optimization process

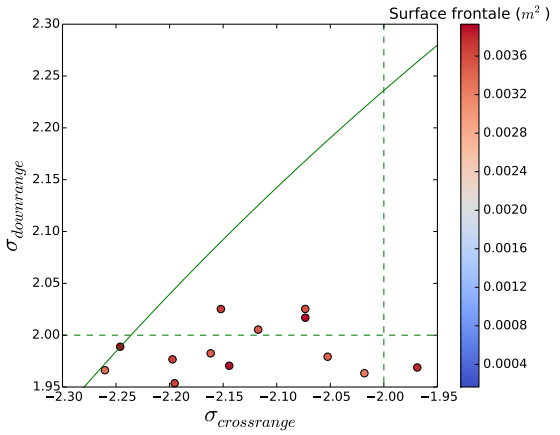

Fig. 20 Zoom on the interest zone of optimization

The nearest solution to the 3σ ellipse is chosen to be evaluated by CFD computations. The aerodynamic conditions at which it will be evaluated are selected as explained in paragraph VI D and illustrated in fig. 11. The process is repeated until the convergence of the impact point is reached.

The optimization process was also run by modelling the aerodynamic coefficients by kriging. The surface of the spoiler is quite the same as the one determined with the MLP model. The time required to optimize the configuration by kriging is 1.5 times higher than by MLP. Since the results are similar, the kriging model of the coefficients is abandoned and only the optimization using MLP model of the coefficients with kriging estimations of the objective and constraint functions is followed.

IX. Conclusion and perspectives

An optimization process was developed, coupling surrogate models and a genetic algorithm to determine the configuration of the spoiler maximizing the lateral deviation of the projectile. Aerodynamic coefficients databases are used in the construction of surrogate models (kriging and MLP). Interpolations based on the models allow the determination of the trajectories of different projectiles at a reduced computational cost. The ability of the methodology to localize promising configurations of the spoiler is demonstrated through a validation study and the research of a 2D correction of the trajectory of the uncontrolled projectile. This optimization was achieved through the calculation of the Expected Improvement based on the estimation of the kriging model associated to the objective function. Response surfaces are also associated to the constraints defined prior to the optimization and are used to modify the EI score of the configurations that do not meet the requirements. The databases are finally enriched at each step of the optimization with CFD evaluations of aerodynamic coefficients of the optimal spoiler.

The methodology was validated on an analytic problem in 2 dimensions constrained by 3 functions. The algorithm was able to localize the 2 zones presenting low values of the function and samples were added in the vicinity of the global optimum.

The optimization problem is run considering the 5 parameters linked to the spoiler. It appears that the time of deployment of the spoiler defines an iso-surface of reference surface in the 5 dimensional parameters. Any combination of this time and value of reference surface leads to a 2D correction of the trajectory. The optimization problem was closed by selecting the time of deployment corresponding to a terminal guidance of the projectile.

In the end, the optimization problem was run with 4 parameters. It is possible to determine a configuration of the spoiler leading to a 2D correction of the trajectory. This configuration is evaluated by CFD and the response surfaces associated to aerodynamic coefficients are refined during the optimization process. The minimization of the distance

between the impact point and the 3σ ellipse allow the correction of more than 99% of the trajectories without an oversizing of the spoiler.

For the future study, a multi-fidelity kriging model is considered by integrating unsteady CFD results to the initial database. Zonal Detached Eddy Simulations (ZDES) of the projectile equipped with a spoiler will be run and would allow a better modelling of the flow around the projectile, especially of the interactions of the spoiler with the base flow.

Acknowledgement

This work was part of the MANEGE II study funded by DGA within the framework of ONERA/Nexter Munitions/ISL cooperation.

References

[1] Dietrich, F., "Simulation numerique du couplage entre la mecanique du vol et l'aerodynamique des projectiles," Ph.D. thesis, Universite de Poitiers, 2003.

[2] Peter, J., Marcelet, M., Burguburu, S., and Pdiroda, V., "Comparison of surrogate models for the actual global optimization of a 2D turbomachinery flow," *Proceedings of the 7th WSEAS International Conference on Simulation, Modelling and Optimization*, 2007, pp. 46 – 51.

[3] Paiva, R. M., Carvalho, A. R. D., Crawford, C., and Suleman, A., "Comparison of Surrogate Models in a Multidisciplinary Optimization Framework for Wing Design," *AIAA Journal*, Vol. 48, No. 5, 2010, pp. 995 – 1006. doi:10.2514/1.45790.

[4] Simpson, T. W., Mauery, T. M., Korte, J. J., and Mistree, F., "Kriging Models for Global Approximation in Simulation-Based Multidisciplinary Design Optimization," *AIAA Journal*, Vol. 39, No. 12, 2001, pp. 2233 – 2241. doi:10.2514/2.1234.

[5] Meunier, M., "Simulation and Optimization of Flow Control Strategies for Novel High-Lift Configurations," *AIAA Journal*, Vol. 47, No. 5, 2009, pp. 1145 – 1157. doi:10.2514/1.38245.

[6] Kanazaki, M., Tanaka, K., Jeong, S., and Yamamoto, K., "Multi-Objective Aerodynamic Exploration of Elements' Setting for High-lift Airfoil Using Kriging Model," *Journal of Aricraft*, Vol. 44, No. 3, 2006, pp. 858 – 864. doi:10.2514/1.25422.

[7] Jeong, S., Murayama, M., and Yamamoto, K., "Efficient Optimization Design Method Using Kriging Model," *Journal of Aircraft*, Vol. 42, No. 2, 2005, pp. 413 – 420. doi:10.2514/1.6386.

[8] Swiler, L. P., Slepoy, R., and Giunta, A., "Evaluation of Sampling Methods in Constructing Response Surface Approximations," *47th AIAA/ASME/ASCE/AHS/ASC Structures, Structural Dynamics, and Materials Conference*, AIAA, 2006. doi:10.2514/6.2006-1827.

[9] Mckay, M. D., Beckman, R. J., and Conover, W. J., "A Comparison of Three Methods for Selecting Values of Input Variables in the Analysis of Output From a Computer Code," *Technometrics*, Vol. 21, No. 2, 1979, pp. 239 – 245. doi:10.2307/1268522.

[10] Morris, M. D., and Mitchell, T. J., "Exploratory designs for domputational experiments," *Journal of Statistical Planning and Inference*, Vol. 43, No. 3, 1995, pp. 381 – 402.

[11] Jones, D. R., Schonlau, M., and Welch, W. J., "Efficient Global Optimization of Expensive Black-Box Functions," *Journal of Global Optimization*, Vol. 13, No. 13, 1998, pp. 455 – 492. doi:10.1023/A:1008306431147.

[12] Sacks, J., Welch, W. J., Mitchell, T. J., and Wynn, H. P., "Design and Analysis of Computer Experiments," *Statistical Sciences*, Vol. 4, No. 4, 1989, pp. 409 – 423.

[13] McCulloch, W. S., and Pitts, W., "A Logical Calculus of the Ideas Immanent in Nervous Activity," *Bulletin of Mathematical Biophysics*, Vol. 5, No. 4, 1943, pp. 115 – 133. doi:10.1007/BF02478259.

[14] Deb, K., "A Fast and Elitist Multiobjective Genetic Algorithm : NSGA-II," *IEEE Transactions on evolutionary computation*, Vol. 6, No. 2, 2002, pp. 182 – 197.

[15] Deb, K., and Kalyanmoy, D., *Multi-Objective Optimization Using Evolutionary Algorithms*, John Wiley & Sons, Inc., New York, NY, USA, 2001.

[16] Voutchkov, I., and Keane, A., *Multi-Objective Optimization Using Surrogates*, Springer Berlin Heidelberg, Berlin, Heidelberg, 2010, pp. 155–175. doi:10.1007/978-3-642-12775-5_7, URL `https://doi.org/10.1007/978-3-642-12775-5_7`.

[17] Simon, F., Deck, S., Guillen, P., Cayzac, R., and Merlen, A., "Zonal-Detached-Eddy Simulation of Projectiles in the Subsonic and Transonic Regimes," *AIAA Journal*, Vol. 45, No. 7, 2007, pp. 1606–1619. doi:10.2514/1.26827, URL https://doi.org/10.2514/1.26827.

[18] Carette, E., Cayzac, R., Zeidler, M., Denis, P., Thépot, R., Garnier, E., Wey, P., Martinez, B., Libsig, M., and Grignon, C., "Innovative Course Correction Devices: MANEGE Program," *29th International Symposium on Ballistics*, Edinburgh, 2016.

[19] Wey, P., Martinez, B., Cayzac, R., Carette, E., Denis, P., and Grignon, C., "2D Course Correction System for Spin-Stabilized Projectiles Using a Spoiler Control Surface," *28th International Symposium on Ballistics*, 2014.

[20] Schonlau, M., "Computer Experiments and Global Optimization," Ph.D. thesis, University of Waterloo, 1997.

[21] Parr, J. M., Keane, A. J., Forrester, A. I., and Holden, C. M., "Infill sampling criteria for surrogate-based optimization with constraint handling," *Engineering Optimization*, Vol. 44, No. 10, 2012, pp. 1147–1166. doi:10.1080/0305215X.2011.637556, URL https://doi.org/10.1080/0305215X.2011.637556.

[22] Wey, P., Corriveau, D., Saitz, T. A., de Ruijter, W., and Strömbäck, P., "BALCO 6/7-DoF TRAJECTORY MODEL," *29th International Symposium on Ballistics*, Vol. 1, 2016, pp. 151 – 162.

[23] Forrester, A. I. J., and Keane, A. J., "Recent advances in surrogate-based optimization," *Progress in Aerospace Sciences*, Vol. 45, No. 1 - 3, 2009, pp. 50 – 79. doi:10.1016/j.paerosci.2008.11.001.

[24] Sasena, M. J., "Flexibility and Efficiency Enhancements for Constrained Global Design Optimization with Kriging Approximations," Ph.D. thesis, University of Michigan, 2002.

[25] Durantin, C., Marzat, J., and Balesdent, M., "Analysis of multi-objective Kriging-based methods for constrained global optimization," *Computational Optimization and Applications*, Vol. 63, No. 3, 2016, pp. 903–926. doi:10.1007/s10589-015-9789-6, URL https://doi.org/10.1007/s10589-015-9789-6.